The functional connectivity status of DMN and its anti-correlated networks across cognitive loads in Clinical High Risk for Psychosis

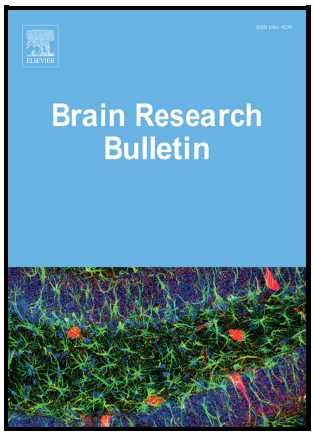

Ling Quan, Xiaoying Sun, Chuan He, Xiao Guo, Ting Ye, Hanxi Wu, Gujing Li, Maria Luisa Bringas-Vega, Sisi Jiang, Dezhong Yao, Cheng Luo

PII: S0361-9230(25)00521-0

DOI: https://doi.org/10.1016/j.brainresbull.2025.111709

Reference: BRB111709

To appear in: *Brain Research Bulletin*

Received date: 29 August 2025
Revised date: 8 December 2025
Accepted date: 25 December 2025

Please cite this article as: Ling Quan, Xiaoying Sun, Chuan He, Xiao Guo, Ting Ye, Hanxi Wu, Gujing Li, Maria Luisa Bringas-Vega, Sisi Jiang, Dezhong Yao and Cheng Luo, The functional connectivity status of DMN and its anti-correlated networks across cognitive loads in Clinical High Risk for Psychosis, *Brain Research Bulletin,* (2025) doi:https://doi.org/10.1016/j.brainresbull.2025.111709

The functional connectivity status of DMN and its anti-correlated networks across cognitive loads in Clinical High Risk for Psychosis

Ling Quan[1,2], Xiaoying Sun[1,2], Chuan He[1,2], Xiao Guo[1,2], Ting Ye[1,2], Hanxi Wu[1,2], Gujing Li[1,2], Maria Luisa Bringas-Vega[2,4], Sisi Jiang[1,2,3], Dezhong Yao[1,2,3], Cheng Luo[1,2,3,5*]

Author affiliations:
1 The Clinical Hospital of Chengdu Brain Science Institute, School of Life Science and Technology, University of Electronic Science and Technology of China, Chengdu 611731, P. R. China
2 China-Cuba Belt and Road Joint Laboratory on Neurotechnology and Brain-Apparatus Communication, University of Electronic Science and Technology of China, Chengdu, 610054, P. R. China
3 Research Unit of NeuroInformation, Chinese Academy of Medical Sciences, 2019RU035, Chengdu, P. R. China
4 Cuban Neuroscience Center, La Habana, Cuba
5 Department of Radiology, The Clinical Hospital of Chengdu Brain Science Institute, University of Electronic Science and Technology of China, Chengdu 611731, P. R. China
Correspondence to: Cheng Luo
Full address: No.2006, Xiyuan Ave, West Hi-Tech Zone, 611731, Chengdu, Sichuan
E-mail: chengluo@uestc.edu.cn

ABSTRACT

The abnormal functional integration of DMN was widely observed in the psychosis. However, few studies focused on DMN in individuals at Clinical High Risk for Psychosis (CHR), especially under different cognitive loads. The present research predominantly focused on DMN and its antagonism with other networks using the functional MRI. To characterize the specificity of cognitive load-dependent antagonism between DMN and its anti-correlated networks in CHR, this study simulated a graded cognitive load continuum by implementing resting-state fMRI (Minimal cognitive load), passive SSVEP task (low cognitive load), and Emotional Face-Matching Task (high cognitive load). There were 36 CHR individuals and 39 healthy controls (HC) enrolled. Static and dynamic functional connectivity (sFC and dFC) were analyzed. The CHR subjects exhibited significantly reduced antagonism between higher-order cortices and DMN under low cognitive condition. Conversely, they demonstrated enhanced antagonism with greater fluctuation under high cognitive condition, likely a compensatory mechanism to maintain cognitive performance. Concurrently, the primary cortex demonstrated compensatory fluctuations during low cognitive load task. The neural signature reflects inefficient neural resource allocation and cognitive flexibility deficits, suggesting that dynamic brain network indicators based on cognitive load may become sensitive biomarkers for the early identification and intervention of CHR.

Keywords: CHR, DMN, antagonism, cognitive load, static functional connectivity, dynamic functional connectivity

1. INTRODUCTION

Research on the clinical outcomes and neural mechanisms of individuals at Clinical High Risk for Psychosis (CHR)(Catalan et al., 2021) is pivotal in psychiatry. Prospective studies demonstrated that 15%-30% of CHR individuals will transition to frank psychosis within two years(Sefik et al., 2023; Zhang et al., 2014), emphasizing the imperative for early intervention. However, from another perspective, the CHR stage also offers a crucial window for observing prodromal neurobiological changes of psychosis(Catalan et al., 2021; Fusar-Poli et al., 2020).

Using resting-state neuroimaging tools, a highly active default mode network (DMN) and an organized anti-correlated network pattern are observed in human brain. This organized pattern is conceptually framed as a phenomenon of antagonism(Fox et al., 2005), a term which refers to the competitive and reciprocal relationship between these two large-scale brain systems. However, the antagonistic relationship might be affected during cognitive tasks, particularly those with high cognitive load(Luo et al., 2016). This phenomenon reflects a brain mechanism whereby functional networks dynamically adjust to allocate cognitive resources efficiently, thereby underpinning cognitive flexibility(Meda et al., 2025). Notably, aberrant static and dynamic functional connectivity between the DMN and its antagonistic networks such as the salience network (SN) and central executive network (CEN) has been identified in neuropsychiatric disorders like schizophrenia and Alzheimer's disease(Dong et al., 2018; Du et al., 2018).Disruptions of this dynamic balance among brain networks may underlie neurocognitive inflexibility in psychiatric disorders, that is, the brain fails to flexibly reconfigure antagonistic relationships among networks according to task requirements(Gonzalez-Castillo et al., 2015; Yin and Kaiser, 2021).

Actually, the characteristic abnormalities of regulatory mechanisms of DMN were observed in CHR individuals(Damme et al., 2019; Dutt et al., 2015). While existing research predominantly focusing on findings from resting-state functional magnetic resonance imaging (fMRI), few studies have systematically integrated multi-modal brain network features across both resting and task-based conditions. There are two critical reasons for us to pay attention on this topic: (1) cognitive flexibility necessitates the integration of intrinsic and task-driven processes(Bouchacourt and Buschman, 2019); (2) as a core network underpinning important cognitive functions such as self-referential processing and episodic memory retrieval(Yeshurun et al., 2021), the neural activity patterns of the DMN exhibit significant spatiotemporal specificity across distinct cognitive states(Smallwood et al., 2021). Therefore, the present study concurrently incorporates resting-state with task-based fMRI under both low and high cognitive loads. This design simulates a dynamic process of varying cognitive loads, aiming to systematically investigate the interaction between functional brain network differences (CHR vs. healthy controls) and task loads, as well as their dynamic association patterns.

2. MATERIALS AND METHODS

2.1 Participants

Participants were recruited from University of Electronic Science and Technology of China, ages 17-20 years. The Institutional Review Board of UESTC for Brain Research approved study protocols under approval number 2019LLYJ08 and all participants provided informed consent.

CHR participants were identified by the Chinese version of the 16-item Prodromal Questionnaire (PQ-16) and should met 6 or more symptoms(Ising et al., 2012; Parabiaghi et al., 2024). Inclusion

criteria were set as: right-handed individuals whose corrected visual acuity can reach the normal level. Exclusion criteria were set as: the individual or their first-degree relatives suffer from psychotic disorder, have congenital or acquired neurodevelopmental delay, have drug dependence or abuse, and have organic brain lesions. In addition, Healthy controls (HC) participants could not have first-degree family history of psychosis, could not have acute anxiety attacks recently, and could not be using psychotropic medication at the time of study.

After excluding participants who were suspected to lie in scale measurement and did not pass MRI quality control standards or with incomplete data, 36 CHR participants and 39 HC were included in the present analyses. Both groups were matched in age and gender.

2.2 Behavioral evaluation

Psychological assessment during the experimental phase was conducted using Self-Rating Depression Scale (SDS) (Zung, 1965), Self-Rating Anxiety Scale (SAS) (Zung, 1971), Interpersonal Reactivity Index - Chinese Version (IRI-C), Emotional Quotient Scale (EQ), Basic Empathy Scale (BES) (Jolliffe and Farrington, 2006), and Perceived Social Support Scale (PSSS) (Blumenthal et al., 1987). This comprehensive assessment evaluated participants' psychological status across multiple domains: depressive symptoms, anxiety levels, psychological impact of life events, interpersonal characteristics and coping styles, emotional competencies, and perceived social support systems. Additionally, the demographic data was also collected including gender, age, and education years.

2.3 Data Acquisition/Scanning

Scanning Parameters. Structural and functional magnetic resonance imaging (MRI) data for both resting-state and task-based conditions were acquired using a 3.0T GE Discovery MR750 scanner. During scanning, all participants were instructed to remain awake, lie supine with arms and legs uncrossed in a natural position, maintain body relaxation and minimize movement. Head movement was minimized using foam padding, and participants wore earplugs for noise attenuation. Functional MRI (fMRI) data were acquired using a T2-weighted gradient-recalled echo-planar imaging (EPI) sequence. Coverage extended from the vertex to the foramen magnum. Acquisition parameters were: repetition time (TR) = 2000ms, echo time (TE) = 30ms, slice thickness = 4mm, field of view (FOV) = 240mm × 240mm, acquisition matrix = 64 × 64, flip angle = 90°, and number of slices = 39(axial). Anatomical T1-weighted images were acquired using a 3-dimensional fast spoiled gradient recalled sequence with the following parameters: slice thickness = 1mm, TR = 8.2ms, TE = 3.2ms, field of view (FOV) = 256mm × 256mm, flip angle = 12°, data matrix = 256 × 256. There were 136 axial slices for each subject.

Design. To investigate differences in brain network characteristics across participant groups under different cognitive loads, we designed resting state and two task conditions. The session commenced with a resting-state fMRI acquisition to establish minimal cognitive load condition (baseline neural activity). Following this, participants underwent two distinct task conditions, including Steady-State Visual Evoked Potential (SSVEP, as low cognitive load condition) and Emotional Face-Matching Task (EFMT, as high cognitive load condition), presented in a counterbalanced order. This randomized sequence was implemented to control for potential order effects and fatigue-related confounds across the participant cohort. To further avoid carryover or interference effects, the T1 scan was strategically placed between the SSVEP and EMFT scans.

In resting-state fMRI protocol, participants were instructed to stare at the cross cursor in the center of the screen, stay awake and try not to think. The scanning time for the resting-state data was 510 seconds, which was 255 time points.

The SSVEP experiment, a passive stimulation task, was selected as the low cognitive load task(Bayram et al., 2011; Dawson, 1954; Herrmann, 2001; Perlstein et al., 2003). Alternating black-and-white images were used to simulate SSVEP, delivering frequency stimulations at 5 Hz, 10 Hz, and 20 Hz respectively (Herrmann, 2001). The experiment employed a block design with task stimulation and rest periods alternating. Stimulation at each frequency was presented three times, with each block lasting 20 seconds. The EFMT—a classic paradigm for investigating the perception, recognition, and processing mechanisms of emotional information—was used to assess differences in brain activity when participants performed a high cognitive load task(Hall et al., 2008). We chose 30 foreign emotional face images from a public affective picture database, comprising 15 angry expression images and 15 fearful expression images. Participants were required to press the button to select the face picture matching the target emotion appeared above. The experiment also included 4 neutral images represented by different elliptical patterns for selecting the target shape. The EFMT consisted of 10 blocks, each lasting 30 seconds and containing 6 images, with emotional stimuli and neutral stimuli presented alternately. The accuracy rate and reaction time of the subjects in completing the tasks were recorded.

MRI processing. The fMRI data were preprocessed with the DPARSF software(Chao-Gan and Yu-Feng, 2010). After removing the initial 5 volumes, we performed slice-timing correction and head motion correction. Then, we normalized the brain images to the Montreal Neurological Institute (MNI) standard space(Ashburner and Friston, 1999). We performed spatial smoothing using a 6-mm Gaussian smoothing kernel. Additionally, linear drifts were removed. After nuisance regression(Friston et al., 1996), we conducted bandpass filtering (0.01–0.10 Hz) to attenuate low-frequency drifts and high-frequency noise. Participants exhibiting excessive head motion (translation exceeding 2.5 mm or rotation exceeding 2.5°) were excluded from this study to ensure data quality.

For both resting-state and task-based fMRI data, a spherical area with a 6-mm radius centered at the MNI coordinates (-5, -49, 40) of the posterior cingulate cortex (PCC)(Fox et al., 2005) was selected as the region of interest (ROI) representing DMN. Seed-based static functional connectivity (sFC) and dynamic functional connectivity (dFC) was computed between the PCC and remained brain voxels. The sFC analysis was performed according to our previous study(Luo et al., 2016). The dFC was computed using the sliding window approach(Allen et al., 2014). Major parameters were set as follows: The window length was 50 TRs, which has shown to be suitable for capturing dynamics in FCs. The window slid in steps of 1 TR, resulting in 201 sliding windows for each subject. The standard deviation (std) of functional connection within each window was calculated to represent temporal variability. Both sFC and dFC measures underwent Fisher's Z-transformation to improve the normality of the observed metrics.

2.4 Statistical analyses

Demographic characteristics of participants were analyzed using IBM SPSS 26.0. Continuous demographic variables were compared using independent samples T test, while categorical variables were assessed with chi-square test.

Functional connectivity differences between CHR and HC groups were examined using the

DPABI Statistical Analysis module. For rest-state FC, T-statistics were calculated for each group with sex, age, and head motion parameters as covariates. Clusters with more than 23 voxels were retained. We checked for two-way interactions between task and diagnostic group using analyses of variance (ANOVA) in sFC and dFC. A Bonferroni correction was used for simple effect analysis after extracting significant interaction effects. Finally, Pearson correlation analyses were conducted between FC values and SDS, SAS, IRI-C, BES, and PSSS scores.

3. RESULTS

3.1 Sample Characteristics

There were no significant differences between groups in age and gender, as well as task performance. All participants were early-stage undergraduates which ensured equivalent years of education. CHR group showed significantly more serious PQ-16 symptoms than controls. There were also significant group differences in SDS, SAS, IRI-C Personal Distress (PD), PSSS, and PSSS friend support (FRS) (Table 1).

As the CHR screening scale, the PQ-16 scale demonstrated good internal consistency, with a Cronbach's α of 0.879 for the item scores (presence/absence) and 0.900 for the distress scores. The PSSS, SAS, and EQ demonstrated acceptable to good internal consistency (Cronbach's $\alpha = 0.891$, 0.715, and 0.692, respectively), while the IRI-C was marginally below the conventional threshold ($\alpha = 0.606$). The SDS and BES scales failed to meet the reliability standards and were excluded from subsequent analyses.

3.2 Resting-state Functional Connectivity Analyses

Separating one-sample t-tests of sFC between the PCC and whole brain for CHR and HC revealed characteristic DMN hyperconnectivity during resting state. DMN regions including bilateral angular gyri, bilateral middle frontal gyri, bilateral superior frontal gyri, and precuneus exhibited significantly positive connectivity with PCC. Conversely, core regions of dorsal attention, ventral attention, and somatomotor networks—specifically bilateral precentral gyri, bilateral supramarginal gyri, and right superior occipital gyrus—showed significantly negative connectivity with PCC (Fig. S1).

In order to find the differences between groups, we first compared the sFC of CHR and HC participants at resting state. There was a significantly weakened effect of CHR group in left middle occipital gyrus (L.MOG) and right postcentral gyrus (R.PoG). GRF-corrected group differences persisted in both voxel-based analyses at $p < 0.005$ threshold and cluster-based analyses at $p < 0.05$ threshold (Fig. 1, Table 2).

We next tested whether the CHR group existed difference dynamic fluctuations compared with HC group. The two-sample t-test displayed that CHR participants had a smaller std of dFC ($p < 0.005$) in orbital middle frontal gyrus (MFGorb) (Fig. 1, Table 2).

3.3 Task-state Functional Connectivity Analyses

Results indicated a significant two-way interaction between task and group ($p < 0.001$) on sFC in right inferior temporal gyrus (R. ITG), bilateral inferior parietal lobules (L.R. IPL), and left superior frontal gyrus (L. SFG). In simple effect analysis (Fig. 4), all these regions exhibited negative connectivity with PCC. Under low cognitive load state (simulated by SSVEP), CHR group showed significant weaker sFC strength than HC group in L. IPL ($F = 4.803$, $p = 0.032$, $\eta^2 = 0.063$) and L.

MFG ($F = 6.253$, $p = 0.015$, $\eta^2 = 0.081$). In contrast, under high cognitive load state (simulated by EFMT), CHR group demonstrated significantly stronger sFC strength than the HC group across all four brain regions (in R.ITG: $F = 13.026$, $p < 0.001$, $\eta^2 = 0.155$; in R.IPL: $F = 4.868$, $p = 0.031$, $\eta^2 = 0.064$; in L.IPL: $F = 10.162$, $p = 0.002$, $\eta^2 = 0.125$; in L. MFG: $F = 4.681$, $p = 0.034$, $\eta^2 = 0.$ 0.062). Additionally, the HC group displayed significant task differences in R. ITG ($p < 0.001$), R. IPL ($p = 0.031$), and L. IPL ($p < 0.001$), while the CHR group showed significant task differences in R. IPL ($p = 0.002$) and L. MFG ($p < 0.0001$).

For dFC, there were significant group-by-task interaction effects ($p < 0.01$) in left superior occipital gyrus (L. SOG) and right medial superior frontal gyrus (R. mSFG) (Fig. 3). Simple effect analysis revealed that in L. SOG, CHR group exhibited significantly greater dFC than the HC group during SSVEP task ($F = 5.268$, $p = 0.025$, $\eta^2 = 0.069$), while significantly smaller during EFMT ($F = 7.267$, $p = 0.009$, $\eta^2 = 0.093$). In R. mSFG, CHR group exhibited significantly greater dFC than the HC group during EFMT ($F = 9.912$, $p = 0.002$, $\eta^2 = 0.122$).

3.4 Correlation Analysis

We investigated the relationship between functional differences of brain network and psychological states of the participants.

For CHR individuals, the significant relationship between FC and scales were only found in the EFMT processing (Fig. 4). Specifically: (1) in R. ITG, the CHR group showed a positive correlation with FAS in PSSS ($r = 0.342$, $p = 0.048$) (Fig. 4(A)). (2) in R. IPL, the CHR group exhibited a positive correlation with FAS in PSSS ($r = 0.376$, $p = 0.028$) (Fig. 4(B)). (3) in L. SFG, the CHR group displayed positive correlations with both FRS in PSSS ($r = 0.368$, $p = 0.032$) (Fig. 4(C)).

Meanwhile, we found several correlations in healthy subjects (Fig. S2). Among multiple behavioral evaluations, only the PSSS scale demonstrated statistically significant correlations with sFC and dFC patterns. These correlations existed in both resting-state and task-based state.

4. Discussion

This study employed different cognitive loads (minimal/low/high) paradigms to systematically investigate functional coordination of brain network in CHR individuals. Here resting state was considered as the condition with minimal cognitive load. Major findings include: under low cognitive load, CHR individuals exhibited reduced antagonism between higher-order cortices and DMN, reflecting constrained adaptive regulation capacity of functional networks; under high cognitive load, CHR maintained cognitive performance through significantly enhanced antagonism and heightened dynamic fluctuations between higher-order cortices and DMN. This phenomenon implied that the dynamic network adaptations may compensate for cognitive constraints in CHR. However, in primary cortices, this kind of compensatory dynamic network fluctuations emerged during low cognitive load but failed under high cognitive load. Consequently, CHR individuals demonstrated cognitive load-dependent specificity in the antagonistic relationship between the DMN and its anti-correlated networks. This neural signature reflects inefficient allocation of neural resource and cognitive flexibility defects in CHR individuals.

Higher-order cortices, serving as the cognitive control hub of the brain, play a pivotal role in neural resource allocation through dynamic antagonism with DMN across resting and task-based states (Douw et al., 2016). This study revealed that higher-order cortices-DMN interactions had hierarchical characteristics dependent on cognitive load. At resting state, CHR exhibited reduced

dFC variability between MFGorb and PCC compared to HC, demonstrating diminished baseline neural flexibility consistent with prior studies (Kaiser et al., 2016; Pelletier-Baldelli et al., 2018). During the low cognitive load task, SSVEP, significantly weakened antagonism of DMN with frontal and parietal lobes in CHR indicated further constrained adaptive regulation capacity of functional networks. Notably, during the high cognitive load task, EFMT, the CHR group exhibited altered functional connectivity patterns in spite of the comparable behavioral performance between groups. Across all higher-order cortical regions exhibiting significant interaction effects, the CHR group demonstrated abnormally enhanced antagonism with DMN alongside significantly elevated dynamic variability. Prior research suggests such hyperconnectivity may reflect compensatory network mechanisms (Wen et al., 2020). In our study, the high cognitive load in emotion task likely forced CHR individuals to over-recruit higher-order cortical resource—via compensatory hyper-antagonism with DMN—to maintain executive function. Thus, such processing patterns under different cognitive load conditions signify inefficient neural resource allocation of CHR. Accumulating evidence from neuroimaging and behavioral investigations supports this perspective. (Fryer et al., 2019; Whitfield-Gabrieli et al., 2009). These early biomarkers of brain network occurred before observable behavioral defects, providing a guiding basis for prospective preventive intervention.

Primary cortices process bottom-up sensory information while DMN implements the top-down filtering regulatory mechanism. Their synergistic effect forms a "gate" for information transmission to higher-order cortices (Adler et al., 1982; Liu et al., 2024; Ronde et al., 2024). In CHR individuals, resting-state demonstrates weakened anti-correlation between DMN and left middle occipital gyrus as well as right postcentral gyrus. During low cognitive load task, the elevated variability emerged. These findings might reflect impaired filtering mechanism of sensory information in the primary cortex which as a “gate” in CHR. With a large amount of redundant information flooding into the higher cortex, the regulatory function of higher-order cortex is led to overload(Dong et al., 2019; Pessoa et al., 2003). For this reason, under low cognitive load, CHR individuals need to make up for the problem of reduced anti-correlation through heightened inter-network fluctuation, so as to ensure sufficient resource allocation for optimized external information processing. As cognitive demands escalate, efficient neural resource utilization becomes critical (Tian et al., 2007). Under high cognitive load, dynamic fluctuation between DMN and primary cortex significantly diminished. Brain resource was prioritized to meet advanced cognitive needs, further highlighting the insufficiency of cognitive resource in CHR. Therefore, these cognitive load-dependent functional changes in primary cortices in CHR individuals may reflect deficits in filtering bottom-up sensory information. If this dynamic filtering process keep failing in the long term, it may trigger a vicious cycle, leading CHR to further develop into schizophrenia spectrum disorders — manifesting as reality distortion and formal thought disorders (Dong et al., 2023; Fryer et al., 2013).

The relationship between participants' brain network characteristics and behavioral scales was also evaluated. Under high cognitive load condition, a positive relationship emerged between PSSS and sFC linking higher-order cortices and DMN. These results suggest that stronger social support may reduce compensatory demands on higher-order cortical networks in CHR individuals. This may potentially be attributed to the role of optimizing attentional control and cognitive strategies played by social support(Mutschler et al., 2022; Wang et al., 2018). Interestingly, healthy participants scored significantly higher on the PSSS scale than CHR, yet no correlations were observed between the frontoparietal network-DMN connectivity and PSSS during the emotion task. This may reflect

the more automated and adaptive emotional processing in healthy individuals(Yeshurun et al., 2021). In contrast, the positive correlation observed in CHR likely reflects a kind of rule-based social strategy acquired from social support systems, which still represents a pathological compensatory mechanism. Overall, perceived social support may serve as a critical psychological resource which plays a vital neuroprotective role in the cognitive functioning of CHR individuals. Future studies could further delineate its specific effective stages and protective scope in the evolution of mental disease.

Several limitations should be considered in our study. First, participants with CHR in this study were recruited from a university population, where comprehensive diagnostic assessments using structured interviews (e.g., SIPS) proved challenging to implement. Thus, reliance solely on the PQ-16 scale for screening may have resulted in relatively milder symptom severity of CHR subjects. Second, the study was not pre-registered, which may introduce potential bias in our analytical approach. However, we have detailed our methodology and analytical plan to maximize transparency. Future confirmatory studies would benefit from a pre-registered protocol. Third, the FC calculation was based on the entire task duration, this mode may affect the extraction accuracy of FC that only represents the task process. Fourth, this study observed that CHR has cognitive load-dependent brain network functional connectivity specificity. It is necessary to conduct longitudinal research, through data from multiple timepoints, to further validate whether the observed specificity can serve as predictive biomarkers for CHR. Future research could also explore whether behavioral training targeted at social support can repair neural plasticity in CHR, facilitating a transformation from pathological compensation to functional rehabilitation.

5. Conclusion

This study reveals a cognitive load-dependent abnormal antagonistic relationship between the DMN and its anti-correlated networks in CHR individuals. Under high cognitive load, higher-order cortices maintained executive function through compensatory antagonistic enhancement with DMN. At minimal and low cognitive load, this compensatory effect emerged in interactions between primary cortices and DMN, potentially reflecting the deficit in dynamic filtering of bottom-up information. In CHR individuals, stronger social support buffered compensatory burden on higher-order cortical networks. These findings provide multi-level evidences for neural dysfunction in the prodromal stage of psychiatric disorders. Dynamic network metrics based on cognitive load differences may serve as sensitive biomarkers for early identification and intervention.

Funding

This work was supported by National Key R&D Programme of China (no. 2024YFE0215100), the National Nature Science Foundation of China (nos 62401124, 62571106, and 82371560), the Project of Science and Technology Department of Sichuan Province (nos 2024YFFK0362, 2023NSFSC0037) and the Fundamental Research Funds for the Central Universities (no. ZYGX2022YGRH017). This study was also supported by a grant from the CAMS Innovation Fund for Medical Sciences (CIFMS; no. 2019-I2M-5-039).

CRediT authorship contribution statement

Ling Quan: Writing – original draft, Formal analysis. **Xiaoying Sun**: Validation, Data curation. **Chuan He**: Data curation. **Xiao Guo**: Data curation. **Ting Ye**: Formal analysis, Visualization. **Hanxi Wu**: Formal analysis. **Gujing Li**: Resources. **María Luisa Bringas Vega**: Writing – review,

revision and editing. **Sisi Jiang**: Methodology, Project administration, Writing – review and editing. **Dezhong Yao**: Writing – review, revision and editing. **Cheng Luo**: Design and Supervision, Writing – review, revision and editing, Conceptualization.

Declaration of Competing Interest

The authors declare no conflicts of interest.

References

Adler, L.E., Pachtman, E., Franks, R.D., Pecevich, M., Waldo, M.C., and Freedman, R. (1982). Neurophysiological evidence for a defect in neuronal mechanisms involved in sensory gating in schizophrenia. Biol Psychiatry 17(6), 639-654.

Allen, E.A., Damaraju, E., Plis, S.M., Erhardt, E.B., Eichele, T., and Calhoun, V.D. (2014). Tracking whole-brain connectivity dynamics in the resting state. Cereb Cortex 24(3), 663-676. https://doi.org/10.1093/cercor/bhs352.

Ashburner, J., and Friston, K.J. (1999). Nonlinear spatial normalization using basis functions. Hum Brain Mapp 7(4), 254-266. https://doi.org/10.1002/(SICI)1097-0193(1999)7:4<254::AID-HBM4>3.0.CO;2-G.

Bayram, A., Bayraktaroglu, Z., Karahan, E., Erdogan, B., Bilgic, B., Ozker, M., Kasikci, I., Duru, A.D., Ademoglu, A., Ozturk, C., et al. (2011). Simultaneous EEG/fMRI analysis of the resonance phenomena in steady-state visual evoked responses. Clin EEG Neurosci 42(2), 98-106. https://doi.org/10.1177/155005941104200210.

Blumenthal, J.A., Burg, M.M., Barefoot, J., Williams, R.B., Haney, T., and Zimet, G. (1987). Social support, type A behavior, and coronary artery disease. Psychosom Med 49(4), 331-340. https://doi.org/10.1097/00006842-198707000-00002.

Bouchacourt, F., and Buschman, T.J. (2019). A Flexible Model of Working Memory. Neuron 103(1), 147-160 e148. https://doi.org/10.1016/j.neuron.2019.04.020.

Catalan, A., Salazar de Pablo, G., Aymerich, C., Damiani, S., Sordi, V., Radua, J., Oliver, D., McGuire, P., Giuliano, A.J., Stone, W.S., et al. (2021). Neurocognitive Functioning in Individuals at Clinical High Risk for Psychosis: A Systematic Review and Meta-analysis. JAMA Psychiatry 78(8), 859-867. https://doi.org/10.1001/jamapsychiatry.2021.1290.

Chao-Gan, Y., and Yu-Feng, Z. (2010). DPARSF: A MATLAB Toolbox for "Pipeline" Data Analysis of Resting-State fMRI. Front Syst Neurosci 4, 13. https://doi.org/10.3389/fnsys.2010.00013.

Damme, K.S.F., Pelletier-Baldelli, A., Cowan, H.R., Orr, J.M., and Mittal, V.A. (2019). Distinct and opposite profiles of connectivity during self-reference task and rest in youth at clinical high risk for psychosis. Human Brain Mapping 40(11), 3254-3264. https://doi.org/10.1002/hbm.24595.

Dawson, G.D. (1954). A summation technique for the detection of small evoked potentials. Electroencephalogr Clin Neurophysiol 6(1), 65-84. https://doi.org/10.1016/0013-4694(54)90007-3.

Dong, D., Yao, D., Wang, Y., Hong, S.J., Genon, S., Xin, F., Jung, K., He, H., Chang, X., Duan, M., et al. (2023). Compressed sensorimotor-to-transmodal hierarchical organization in schizophrenia. Psychol Med 53(3), 771-784. https://doi.org/10.1017/S0033291721002129.

Dong, D.B., Duan, M.J., Wang, Y.L., Zhang, X.X., Jia, X.Y., Li, Y.J., Xin, F., Yao, D.Z., and Luo, C. (2019). Reconfiguration of Dynamic Functional Connectivity in Sensory and Perceptual System in Schizophrenia. Cerebral Cortex 29(8), 3577-3589. https://doi.org/10.1093/cercor/bhy232.

Dong, D.B., Wang, Y.L., Chang, X.B., Luo, C., and Yao, D.Z. (2018). Dysfunction of Large-Scale Brain Networks in Schizophrenia: A Meta-analysis of Resting-State Functional Connectivity. Schizophrenia Bull 44(1), 168-181. https://doi.org/10.1093/schbul/sbx034.

Douw, L., Wakeman, D.G., Tanaka, N., Liu, H., and Stufflebeam, S.M. (2016). State-dependent variability of dynamic functional connectivity between frontoparietal and default networks relates to cognitive flexibility. Neuroscience 339, 12-21. https://doi.org/10.1016/j.neuroscience.2016.09.034.

Du, Y., Fryer, S.L., Fu, Z., Lin, D., Sui, J., Chen, J., Damaraju, E., Mennigen, E., Stuart, B., Loewy, R.L., et al. (2018). Dynamic functional connectivity impairments in early schizophrenia and clinical high-risk for psychosis. Neuroimage 180(Pt B), 632-645. https://doi.org/10.1016/j.neuroimage.2017.10.022.

Dutt, A., Tseng, H.H., Fonville, L., Drakesmith, M., Su, L., Evans, J., Zammit, S., Jones, D., Lewis, G., and David, A.S. (2015). Exploring neural dysfunction in 'clinical high risk' for psychosis: a quantitative review of fMRI studies. J Psychiatr Res 61, 122-134. https://doi.org/10.1016/j.jpsychires.2014.08.018.

Fox, M.D., Snyder, A.Z., Vincent, J.L., Corbetta, M., Van Essen, D.C., and Raichle, M.E. (2005). The human brain is intrinsically organized into dynamic, anticorrelated functional networks. Proc Natl Acad Sci U S A 102(27), 9673-9678. https://doi.org/10.1073/pnas.0504136102.

Friston, K.J., Williams, S., Howard, R., Frackowiak, R.S., and Turner, R. (1996). Movement-related effects in fMRI time-series. Magn Reson Med 35(3), 346-355. https://doi.org/10.1002/mrm.1910350312.

Fryer, S.L., Roach, B.J., Ford, J.M., Donaldson, K.R., Calhoun, V.D., Pearlson, G.D., Kiehl, K.A., Srihari, V.H., McGlashan, T.H., Woods, S.W., et al. (2019). Should I Stay or Should I Go? FMRI Study of Response Inhibition in Early Illness Schizophrenia and Risk for Psychosis. Schizophr Bull 45(1), 158-168. https://doi.org/10.1093/schbul/sbx198.

Fryer, S.L., Woods, S.W., Kiehl, K.A., Calhoun, V.D., Pearlson, G.D., Roach, B.J., Ford, J.M., Srihari, V.H., McGlashan, T.H., and Mathalon, D.H. (2013). Deficient Suppression of Default Mode Regions during Working Memory in Individuals with Early Psychosis and at Clinical High-Risk for Psychosis. Front Psychiatry 4, 92. https://doi.org/10.3389/fpsyt.2013.00092.

Fusar-Poli, P., Salazar de Pablo, G., Correll, C.U., Meyer-Lindenberg, A., Millan, M.J., Borgwardt, S., Galderisi, S., Bechdolf, A., Pfennig, A., Kessing, L.V., et al. (2020). Prevention of Psychosis: Advances in Detection, Prognosis, and Intervention. JAMA Psychiatry 77(7), 755-765. https://doi.org/10.1001/jamapsychiatry.2019.4779.

Gonzalez-Castillo, J., Hoy, C.W., Handwerker, D.A., Robinson, M.E., Buchanan, L.C., Saad, Z.S., and Bandettini, P.A. (2015). Tracking ongoing cognition in individuals using brief, whole-brain functional connectivity patterns. Proc Natl Acad Sci U S A 112(28), 8762-8767. https://doi.org/10.1073/pnas.1501242112.

Hall, J., Whalley, H.C., McKirdy, J.W., Romaniuk, L., McGonigle, D., McIntosh, A.M., Baig, B.J., Gountouna, V.E., Job, D.E., Donaldson, D.I., et al. (2008). Overactivation of fear systems to neutral faces in schizophrenia. Biol Psychiatry 64(1), 70-73. https://doi.org/10.1016/j.biopsych.2007.12.014.

Herrmann, C.S. (2001). Human EEG responses to 1-100 Hz flicker: resonance phenomena in visual cortex and their potential correlation to cognitive phenomena. Exp Brain Res 137(3-4), 346-353. https://doi.org/10.1007/s002210100682.

Ising, H.K., Veling, W., Loewy, R.L., Rietveld, M.W., Rietdijk, J., Dragt, S., Klaassen, R.M., Nieman, D.H., Wunderink, L., Linszen, D.H., et al. (2012). The validity of the 16-item version of the Prodromal Questionnaire (PQ-16) to screen for ultra high risk of developing psychosis in the general help-seeking population. Schizophr Bull 38(6), 1288-1296. https://doi.org/10.1093/schbul/sbs068.

Jolliffe, D., and Farrington, D.P. (2006). Development and validation of the Basic Empathy Scale. J Adolesc 29(4), 589-611. https://doi.org/10.1016/j.adolescence.2005.08.010.

Kaiser, R.H., Whitfield-Gabrieli, S., Dillon, D.G., Goer, F., Beltzer, M., Minkel, J., Smoski, M., Dichter, G., and Pizzagalli, D.A. (2016). Dynamic Resting-State Functional Connectivity in Major Depression. Neuropsychopharmacology 41(7), 1822-1830. https://doi.org/10.1038/npp.2015.352.

Liu, Y., Zhang, J., Jiang, Z., Qin, M., Xu, M., Zhang, S., and Ma, G. (2024). Organization of corticocortical and thalamocortical top-down inputs in the primary visual cortex. Nat Commun 15(1), 4495. https://doi.org/10.1038/s41467-024-48924-8.

Luo, C., Yang, F., Deng, J.Y., Zhang, Y.D., Hou, C.Y., Huang, Y., Cao, W.F., Wang, J.J., Xiao, R.H., Zeng, N.L., et al. (2016). Altered functional and effective connectivity in anticorrelated intrinsic networks in children with benign childhood epilepsy with centrotemporal spikes. Medicine 95(24). https://doi.org/ARTN e3831
10.1097/MD.0000000000003831.

Meda, N., Baggio, M., Collantoni, E., and Sambataro, F. (2025). Whole-brain functional neuroimaging correlates of cognitive flexibility impairments in people with mental disorders: A transdiagnostic coordinate-based meta-analysis. Eur Neuropsychopharmacol 93, 40-50. https://doi.org/10.1016/j.euroneuro.2025.01.009.

Mutschler, C., Lichtenstein, S., Yan, S., Blair, F., Davidson, L., Mihalakakos, G., and Kidd, S.A. (2022). Personal recovery in the postdischarge period for individuals with schizophrenia spectrum diagnoses: The role of community integration and social support. Psychiatr Rehabil J 45(2), 176-182. https://doi.org/10.1037/prj0000513.

Parabiaghi, A., Rossi, A.A., Castelnovo, A., Del Fabro, L., Mannarini, S., Percudani, M.E., and team, C.C.M.P. (2024). The Italian version of the 16-item Prodromal Questionnaire (PQ-16) and its psychometric features in help-seeking ultra-high-risk subjects and in the general population. Early Interv Psychiatry 18(10), 814-827. https://doi.org/10.1111/eip.13516.

Pelletier-Baldelli, A., Andrews-Hanna, J.R., and Mittal, V.A. (2018). Resting state connectivity dynamics in individuals at risk for psychosis. J Abnorm Psychol 127(3), 314-325. https://doi.org/10.1037/abn0000330.

Perlstein, W.M., Cole, M.A., Larson, M., Kelly, K., Seignourel, P., and Keil, A. (2003). Steady-state visual evoked potentials reveal frontally-mediated working memory activity in humans. Neurosci Lett 342(3), 191-195. https://doi.org/10.1016/s0304-3940(03)00226-x.

Pessoa, L., Kastner, S., and Ungerleider, L.G. (2003). Neuroimaging studies of attention: from modulation of sensory processing to top-down control. J Neurosci 23(10), 3990-3998. https://doi.org/10.1523/JNEUROSCI.23-10-03990.2003.

Ronde, M., van der Zee, E.A., and Kas, M.J.H. (2024). Default mode network dynamics: An integrated neurocircuitry perspective on social dysfunction in human brain disorders. Neurosci Biobehav Rev 164, 105839. https://doi.org/10.1016/j.neubiorev.2024.105839.

Sefik, E., Boamah, M., Addington, J., Bearden, C.E., Cadenhead, K.S., Cornblatt, B.A., Keshavan, M.S., Mathalon, D.H., Perkins, D.O., Stone, W.S., et al. (2023). Sex- and Age-Specific Deviations in Cerebellar Structure and Their Link With Symptom Dimensions and Clinical Outcome in Individuals

at Clinical High Risk for Psychosis. Schizophr Bull 49(2), 350-363. https://doi.org/10.1093/schbul/sbac169.

Smallwood, J., Bernhardt, B.C., Leech, R., Bzdok, D., Jefferies, E., and Margulies, D.S. (2021). The default mode network in cognition: a topographical perspective. Nat Rev Neurosci 22(8), 503-513. https://doi.org/10.1038/s41583-021-00474-4.

Tian, L., Jiang, T., Liu, Y., Yu, C., Wang, K., Zhou, Y., Song, M., and Li, K. (2007). The relationship within and between the extrinsic and intrinsic systems indicated by resting state correlational patterns of sensory cortices. Neuroimage 36(3), 684-690. https://doi.org/10.1016/j.neuroimage.2007.03.044.

Wang, J., Mann, F., Lloyd-Evans, B., Ma, R., and Johnson, S. (2018). Associations between loneliness and perceived social support and outcomes of mental health problems: a systematic review. BMC Psychiatry 18(1), 156. https://doi.org/10.1186/s12888-018-1736-5.

Wen, X., He, H., Dong, L., Chen, J., Yang, J., Guo, H., Luo, C., and Yao, D. (2020). Alterations of local functional connectivity in lifespan: A resting-state fMRI study. Brain Behav 10(7), e01652. https://doi.org/10.1002/brb3.1652.

Whitfield-Gabrieli, S., Thermenos, H.W., Milanovic, S., Tsuang, M.T., Faraone, S.V., McCarley, R.W., Shenton, M.E., Green, A.I., Nieto-Castanon, A., LaViolette, P., et al. (2009). Hyperactivity and hyperconnectivity of the default network in schizophrenia and in first-degree relatives persons with schizophrenia. P Natl Acad Sci USA 106(11), 4572-4572. https://doi.org/10.1073/pnas.0900938106.

Yeshurun, Y., Nguyen, M., and Hasson, U. (2021). The default mode network: where the idiosyncratic self meets the shared social world. Nat Rev Neurosci 22(3), 181-192. https://doi.org/10.1038/s41583-020-00420-w.

Yin, D., and Kaiser, M. (2021). Understanding neural flexibility from a multifaceted definition. Neuroimage 235, 118027. https://doi.org/10.1016/j.neuroimage.2021.118027.

Zhang, T., Li, H., Woodberry, K.A., Seidman, L.J., Zheng, L., Li, H., Zhao, S., Tang, Y., Guo, Q., Lu, X., et al. (2014). Prodromal psychosis detection in a counseling center population in China: an epidemiological and clinical study. Schizophr Res 152(2-3), 391-399. https://doi.org/10.1016/j.schres.2013.11.039.

Zung, W.W. (1965). A Self-Rating Depression Scale. Arch Gen Psychiatry 12, 63-70. https://doi.org/10.1001/archpsyc.1965.01720310065008.

Zung, W.W. (1971). A rating instrument for anxiety disorders. Psychosomatics 12(6), 371-379. https://doi.org/10.1016/S0033-3182(71)71479-0.

Table 1. Demographics of Clinical High Risk for Psychosis (CHR) and Healthy Control (HC)

	CHR (*n*=36)	HC (*n*=39)	*t/U*	*P*
Gender (male/female)	28/8	31/8	—	0.83
Age (years)	18.42(0.87)	18.56(0.68)	-0.819	0.42
PQ-16	9.00(2.78)	1.51(1.36)	14.69	0.00*
SAS	49.72(11.21)	37.71(4.82)	5.95	0.00*
IRI-C[a]	72.81(7.62)	69.83(6.91)	1.78	0.08

PD	18.08(3.51)	15.21(2.88)	3.90	0.00*
FS	16.89(3.31)	17.87(2.88)	-1.38	0.17
EC	19.42(3.20)	17.77(2.95)	2.32	0.23
PT	18.42(2.77)	19.05(2.48)	-1.05	0.30
EQ	145.78(11.69)	149.63(8.48)	-1.62	0.11
PSSS	58.31(10.52)	64.18(10.15)	-2.41	0.02*
FAS	19.58(3.92)	20.79(4.69)	-1.20	0.24
FRS	19.14(4.58)	22.08(3.63)	-3.00	0.00*
SOS	19.58(4.18)	21.26(3.90)	-1.79	0.08
EFMT accuracy rate[U]	0.84(0.10)	0.84(0.07)	468	0.56
EFMT reaction time (ms)[U]	1770.72(372.06)	1711.92(323.87)	453	0.44

[a]IRI-C is including four dimensions: Personal Distress (PD), Fantasy (FS), Empathy Concern (EC), and Perspective Taking (PT).

[c]PSSS is including two dimensions: Family Support (FAS), Friends Support (FRS), and Significant Others Support (SOS).

*Significant test, P ≤ .05. Among healthy controls, one showed outlier scores on the PSSS scale. This outlier was excluded from statistical analyses.

Table 2. Detailed data of the three significantly different clusters

Regions	Peak MNI coordinate			Cluster sizes	Peak intensity (t value)
	X	Y	Z		
Left middle occipital gyrus	-36	-90	-9	24	3.27
Right postcentral gyrus	33	-36	45	23	3.41
Orbital middle frontal gyrus	-45	45	-9	26	-3.97

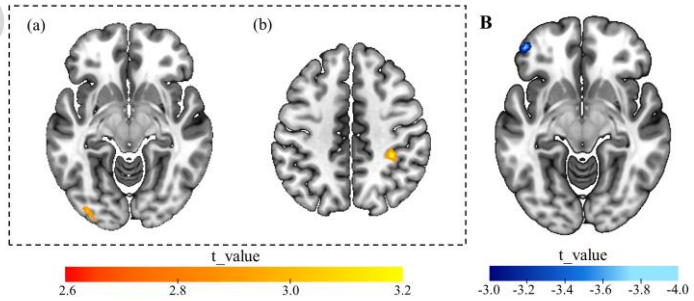

Fig. 1. (A) Two-sample t-test across voxels (GRF corrected, voxel-level p < 0.005 and cluster-level p < 0.05) of resting-state sFC in the pair of groups: (a) left middle occipital gyrus, (b) right postcentral gyrus. (B) Two-sample t-test across voxels (p < 0.005, cluster size > 23) of resting-state dFC in the pair of groups: orbital middle frontal gyrus. The color bars represent t-values.

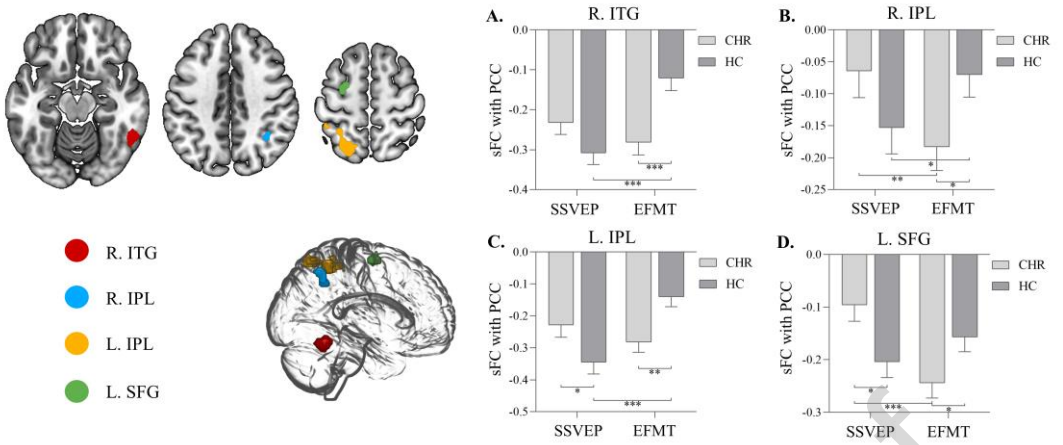

Fig. 2. Significant interaction effects between group and task for sFC ($p < 0.001$). (A) Right inferior temporal gyrus (R. ITG), (B) Right inferior parietal lobule (R. IPL), (C) Left inferior parietal lobule (L. IPL), (D) Left superior frontal gyrus (L. SFG). *Significant test, $p \leq .05$. **Significant test, $p \leq .01$. ***Significant test, $p \leq .001$.

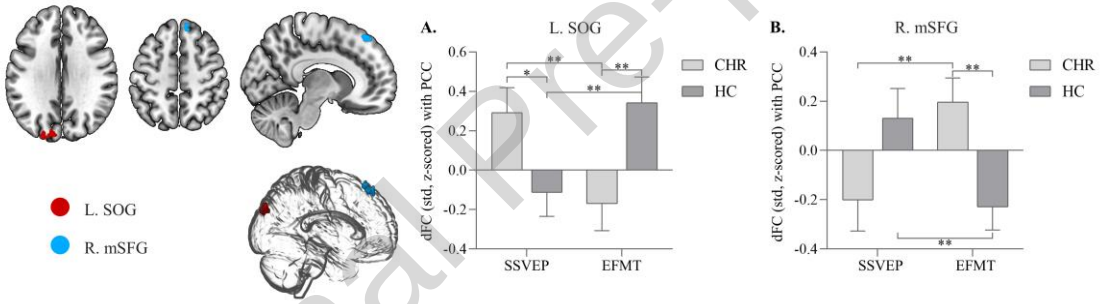

Fig. 3. Significant interaction effects between group and task for dFC ($p < 0.01$). (A) Left superior occipital gyrus (L. SOG), (B) Right medial superior frontal gyrus (R. mSFG). *Significant test, $p \leq .05$. **Significant test, $p \leq .01$.

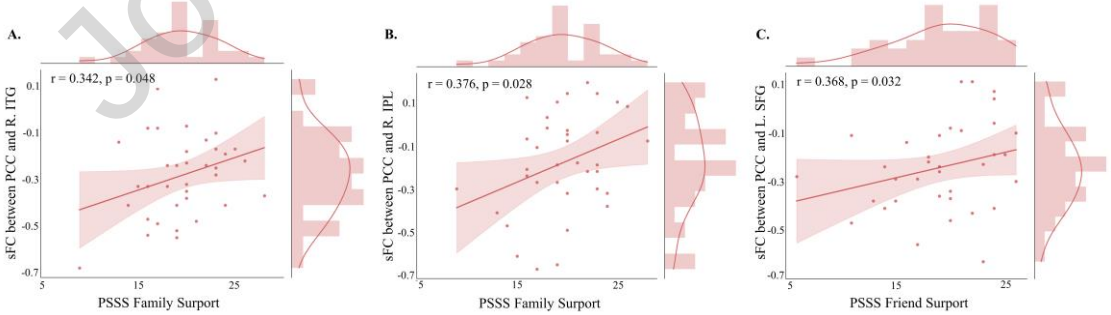

Fig. 4. Correlations between PSSS scores and static functional connectivity (sFC) during the Emotional Face-Matching Task (EFMT) in CHR group.

Declaration of Competing Interest

The authors declare that they have no known competing financial interests or personal relationships that could have appeared to influence the work reported in this paper.

Highlights

- The specific antagonism was observed in CHR under different cognitive loads.
- The antagonism between higher-order cortices and DMN enhanced with greater fluctuation under high cognitive condition.
- The primary cortex demonstrated compensatory fluctuations during low cognitive load task.
- Perceived social support may serve as a critical psychological resource in the cognitive functioning of CHR.